Infrared Spectra of P_4O_6, P_4O_7, P_4O_8, P_4O_9, and P_4O_{10} in Solid Argon

Zofia Mielke[†] **and Lester Andrews***

Chemistry Department, University of Virginia, Charlottesville, Virginia 22901 *(Received: September 1, 1988)*

P_4O_6 was reacted with oxygen atoms (^{16}O and ^{18}O) obtained from ozone photolysis and discharge of oxygen. The P_4O_{7-10} and $P_4O_6{}^{18}O_{1-4}$ products were trapped in solid argon and examined by infrared spectroscopy. The spectra of the four higher oxides support a central P_4O_6 cage structure with additional terminal $P{=}^{16}O$ or $P{=}^{18}O$ bonds. The $P{=}^{16}O$ and $P{=}^{18}O$ vibrations are identified in four higher oxides, and assignments are proposed for several of the more intense P_4O_6 cage absorptions.

Introduction

Two phosphorus oxides have been well characterized, P_4O_6 and P_4O_{10}; several detailed structural and vibrational analyses have been reported.[1-5] Thermal decomposition of P_4O_6 or P_4O_{10} and oxidation of P_4O_6 lead to the intermediate oxides P_4O_7, P_4O_8, and P_4O_9.[6-10] These intermediate oxides have been prepared in mixed crystal phases[6-8] and from the vaporization of solid P_4O_{10},[9] but only P_4O_7 has been isolated in the pure state.[10] Structures of the P_4O_{6-10} oxides have been determined by electron diffraction[1,2] and X-ray investigations.[11] These molecules have the same basic structure with four P atoms connected by six bridging O atoms to form an adamantane-like cage and one, two, three, or four additional O atoms in terminal positions on the pentavalent phosphorus atoms. Although methods of preparation and structure of the intermediate P_4O_{7-9} oxides are known, no detailed vibrational study has been reported; only absorptions of P_4O_7 in solution and Raman spectra of the solid have been listed.[10] Several new lower oxides of phosphorus have been identified and characterized in this laboratory from matrix reactions of P_4 with oxygen atoms.[12] In this paper we report infrared studies of the controlled matrix reaction of P_4O_6 with O atoms and infrared spectroscopic characterization of the P_4O_{7-9} oxides.

Experimental Section

The cryogenic matrix system, ozone preparation, and matrix photolysis have been described previously.[13-16] The P_4O_6 sample was prepared by J. L. Mills; the matrix infrared spectrum was free of impurity absorptions. Ozone was prepared as described previously[14] using normal, 55%, and 98% ^{18}O-enriched oxygen gas. Ozone and P_4O_6 vapor were diluted with argon and codeposited through two separate spray-on lines. The matrix ratio for ozone was varied between 75/1 and 100/1. The approximate matrix ratio for P_4O_6 was between 200/1 and 300/1 with uncertainty due to desorption from the container walls. Both gases were codeposited at 15 ± 2 K for approximately 3 h, the samples were photolyzed with filtered mercury arc radiation, and spectra were recorded on a Perkin-Elmer 983 infrared spectrophotometer system before and after each irradiation. Frequency accuracy is ±0.5 cm^{-1}.

A discharged argon/oxygen mixture (50/1 and 100/1) was also codeposited with Ar/P_4O_6 mixture. A 6-mm o.d. quartz tube was used to direct the flow of discharged Ar/O_2 mixture onto the cold window. Two different microwave discharge (Evenson-Broida cavity, Burdick Model MW 200, 375-W diathermy) conditions were employed: the first experiments employed low microwave power (20–30%), and the second studies used high microwave power (70–80%).[12]

Results and Discussion

Oxidation of P_4O_6 leads to a mixture of P_4O_{7-9} oxides.[8] Identification of bands due to specific P_4O_7, P_4O_8, and P_4O_9 oxides requires several spectra where the proportions of all oxides differ significantly. When P_4O_6 is reacted with oxygen atoms in the matrix, the proportions of a specific oxide depend on the relative concentration of P_4O_6 and oxygen atoms. In the two series of experiments that have been carried out, the sources of the oxygen atoms were ozone photolysis and the discharged argon/oxygen mixture. The relative concentration of P_4O_6 and oxygen atoms was controlled in three different ways: (a) varying the initial relative concentration of Ar/O_3 or Ar/O_2 with respect to Ar/P_4O_6; (b) using filtered radiation and prolonged photolysis time of a matrix of defined $Ar{:}O_3{:}P_4O_6$ concentration (the first set of experiments); (c) applying low microwave power (20–30%) and high microwave power (70–80%) discharge glow (the second set of experiments).

Figure 1 shows an argon matrix infrared spectrum of P_4O_6. Three strong bands were observed at 952.7, 640.6, and 405.2 cm^{-1}, and these are assigned as the three F_2 modes of molecular P_4O_6 in agreement with infrared and Raman spectra of P_4O_6 in solution and gas phase.[3,4] The two bands at 952.7 and 640.6 cm^{-1} are accompanied by weak shoulders at 962.3, 957.9, 956.2, 946.8, 936.4 cm^{-1} and 644.5, 634.4, 631.1 cm^{-1}, respectively, which are concentration dependent and are most probably due to higher aggregates and/or different matrix sites. The weak bands at 1023.6 and at ca. 1290, 1275 cm^{-1} (the bands show some structure with subpeaks at 1293.0, 1290.3, 1288.7 and 1275.3, 1272.7 cm^{-1}, respectively) are assigned to combination modes in agreement with previous studies.[3]

Figure 2a–d shows the infrared spectra in the spectral region 1440–1340 cm^{-1}, which is characteristic of terminal P=O stretching modes, for the matrix obtained by codeposition of Ar/P_4O_6 and Ar/O_3 = 150/1 samples followed by matrix photolysis: after 20-min photolysis using 420-nm filter (Figure 2a) and after 10, 30, and 65-min full arc photolysis (Figure 2b–d). Figure 2e presents the spectrum of the matrix obtained by codeposition of Ar/P_4O_6 and Ar/O_3 = 75 after 55-min full arc photolysis. From the evolution of the a–d spectra, i.e., the change in relative band intensities with prolonged photolysis time, one can conclude that four different species containing P=O bands are present in the matrix samples. The bands due to different species are marked as A, B, C, and D. The preliminary assignment of these bands is straightforward as the oxidation of P_4O_6 oxide

[†] On leave from Institute of Chemistry, Wroclaw University, Wroclaw, Poland.

(1) Beagley, B.; Cruickshank, D. W. J.; Hewitt, T. G.; Haaland, A. *Trans. Faraday Soc.* **1967**, *63*, 836.
(2) Beagley, B.; Cruickshank, D. W. J.; Hewitt, T. G.; Jost, K. H. *Trans. Faraday Soc.* **1969**, *65*, 1219.
(3) Chapman, A. C. *Spectrochim. Acta* **1968**, *24A*, 1687.
(4) Beattie, I. R.; Livingston, K. M. S.; Ozin, G. A.; Reynolds, D. J. *J. Chem. Soc. A* **1970**, 449.
(5) Cyvin, S. J.; Cyvin, B. N. *Z. Naturforsch. A* **1971**, *26*, 901.
(6) Thilo, E.; Heinz, D.; Jost, K. H. *Angew. Chem.* **1964**, *76*, 229.
(7) Heinz, D. *Z. Anorg. Allg. Chem.* **1965**, *336*, 137.
(8) Heinz, D.; Rienitz, H.; Radeck, D. *Z. Anorg. Allg. Chem.* **1971**, *383*, 120.
(9) Muenow, D. W.; Uy, O. M.; Margrave, J. L. *J. Inorg. Nucl. Chem.* **1970**, *32*, 3459.
(10) Walker, M. L.; Mills, J. L. *Synth. React. Inorg. Met.-Org. Chem.* **1975**, *5*, 29.
(11) Jost, K. H.; Schneider, M. *Acta Crystallogr.* **1981**, *B37*, 222.
(12) Andrews, L.; Withnall, R. *J. Am. Chem. Soc.* **1988**, *110*, 5606.
(13) Andrews, L. *J. Chem. Phys.* **1971**, *54*, 4935.
(14) Andrews, L.; Spiker, R. C., Jr. *J. Phys. Chem.* **1972**, *76*, 3208.
(15) Kelsall, B. J.; Andrews, L. *J. Chem. Phys.* **1982**, *76*, 5005.
(16) Withnall, R.; Hawkins, M.; Andrews, L. *J. Phys. Chem.* **1986**, *90*, 575.

0022-3654/89/2093-2971$01.50/0

TABLE I: Observed Vibrational Frequencies (cm^{-1}) for P_4O_n (n = 6–10) Species

	P_4O_7		P_4O_8		P_4O_9		P_4O_{10}		
P_4O_6	^{16}O	^{18}O[a]	^{16}O	^{18}O	^{16}O	^{18}O	^{16}O	^{18}O	assignment
	1379.4	1338.2	1401.6	1359.9	1406.4[e]	1364.2			P=O stretch; A_1[b,c]
			1384.7	1339.8	1397.8	1353.8	1407.9	1365.6	P=O stretch; B_2, E, F_2 in P_4O_{8-10}
952.7	984.8[d]		1004.3	1003.4	1019.4	1018.3	1025.5		P_4O_6 cage modes (F_2 in P_4O_6, P_4O_{10})
	976.3	972 sh	995.9	991.5	1011.9	1010.4			
	966.4	970.1			1005.7	1000.5			
640.6	653.5	650.6	683.7	681.3	706		766.9	763.8	P_4O_6 cage modes (F_2 in P_4O_6, P_4O_{10})
	649.6	648.9	669.3[e]						
	634.6	632.5							
	625.9	624.7	614.5	611.2					P_4O_6 cage modes, A_1
	537.5	534.9	556	554.1	563.4				P=O bending
405.2	427.6	426.7	440.4	439.2	431		412		P_4O_6 cage modes (F_2 in P_4O_6, P_4O_{10})
	391.0	387.1							

[a] Only the terminal oxygen atoms in the P_4O_{7-10} species are substituted by ^{18}O. [b] A few more bands occurred in the P=O stretch region which are assigned to molecular aggregates; these are the 1362.2-, 1390.1-cm^{-1} bands corresponding to perturbed P=O stretch in P_4O_7, P_4O_8 species and 1334.3-, 1332.9-cm^{-1} bands corresponding to perturbed P=^{18}O in $P_4O_6{}^{18}O$ species. [c] In the spectra of $^{16,18}O_3$ experiment two additional bands were identified at 1395.7, 1345.4 cm^{-1} due to P=O stretch in $P_4O_6{}^{16}O^{18}O$. [d] The 984.8-cm^{-1} band has three shoulders at 988.9, 987.1, 981.6 cm^{-1}. [e] Identified with less confidence; another weak band at 1422 cm^{-1} is probably due to a combination band of P_4O_9.

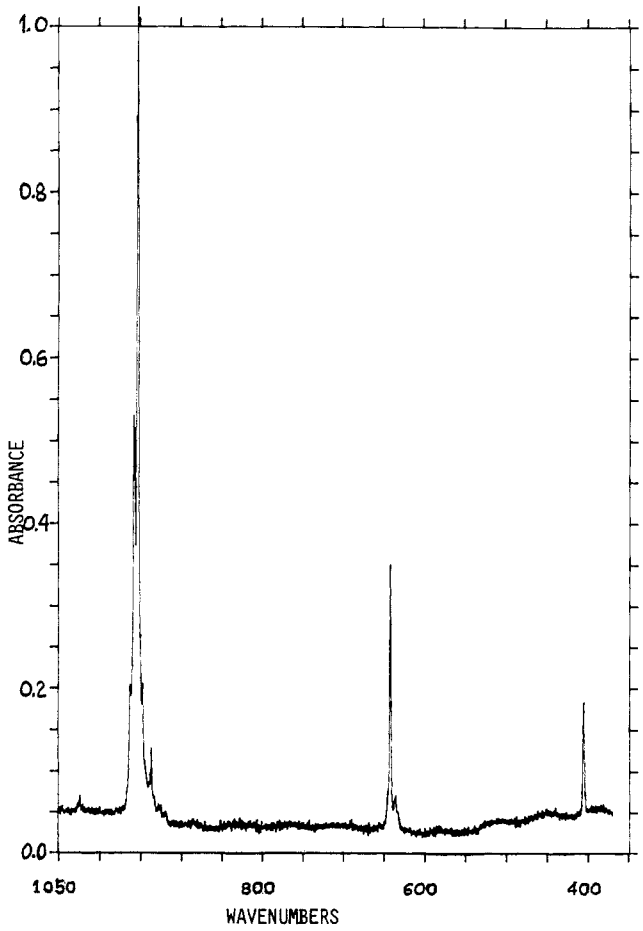

Figure 1. Argon matrix infrared spectrum of P_4O_6 (the Ar/P_4O_6 concentration was between 300/1 and 200/1; the same sample was used in all experiments).

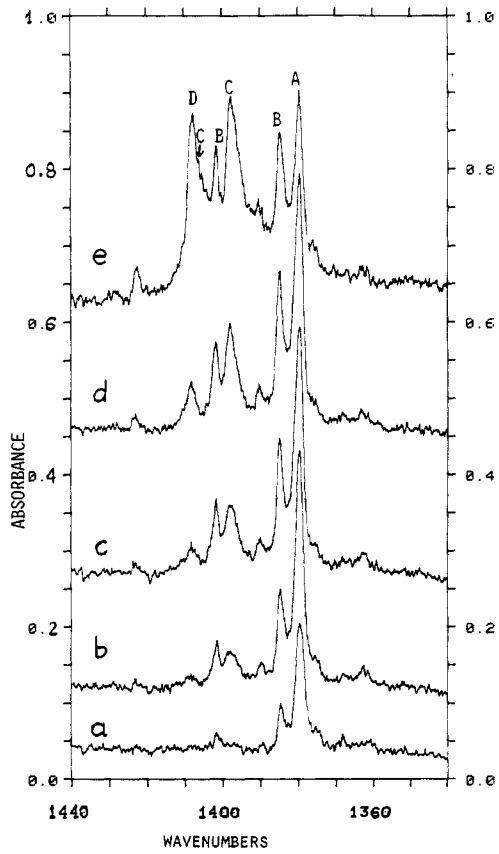

Figure 2. Infrared spectra in the P=O stretching region of a matrix $Ar/P_4O_6 + Ar/^{16}O_3$ = 150/1 after 20-min photolysis using a 420-nm filter (a) and after 10-, 30-, 65-min full arc photolysis (b–d). (e) Infrared spectrum of a matrix $Ar/P_4O_6 + Ar/^{18}O_3$ = 75/1 after 55-min full arc photolysis.

leads to P_4O_{7-10} oxides. Figures 3 and 4 present the spectra of the same matrices in the 1070–920- and the 800–400-cm^{-1} regions, which are characteristic of P_4O_6 cage modes. The intensities of the bands appearing in these regions correlate well with corresponding A, B, C, and D absorptions in the P=O terminal region and are marked in the same way.

Figure 5a,b presents spectra of the P=O region for matrices obtained by codeposition of Ar/P_4O_6 with Ar/O_2 = 100/1 and Ar/O_2 = 50/1 samples subjected to low-power and high-power microwave discharge, respectively. These spectra as well as the spectra in the region of P_4O_6 cage modes correspond closely to the spectra of matrices obtained for photolyzed $Ar/P_4O_6 + Ar/O_3$ matrices. The positions of new bands appearing after reaction of P_4O_6 with oxygen atoms are listed in Table I.

Experiments were done with ^{18}O-enriched ozone prepared from 98 and 55% enriched oxygen, and the resulting spectra are shown in Figures 6 and 7. Large shifts were observed for the terminal modes and small shifts for the cage modes as listed in Table I.

Structures of the P_4O_7, P_4O_8, P_4O_9, and P_4O_{10} oxides have been determined by electron diffraction[1,2] and X-ray investigations;[11] their point groups are C_{3v}, C_{2v}, C_{3v}, and T_d, respectively. Table II summarizes the symmetry and activity expected for both terminal and cage modes.

Terminal P=O Modes

^{16}O Species. In the region of terminal P=O stretching modes eight bands are identified at 1362.2, 1379.4, 1384.7, 1390.1,

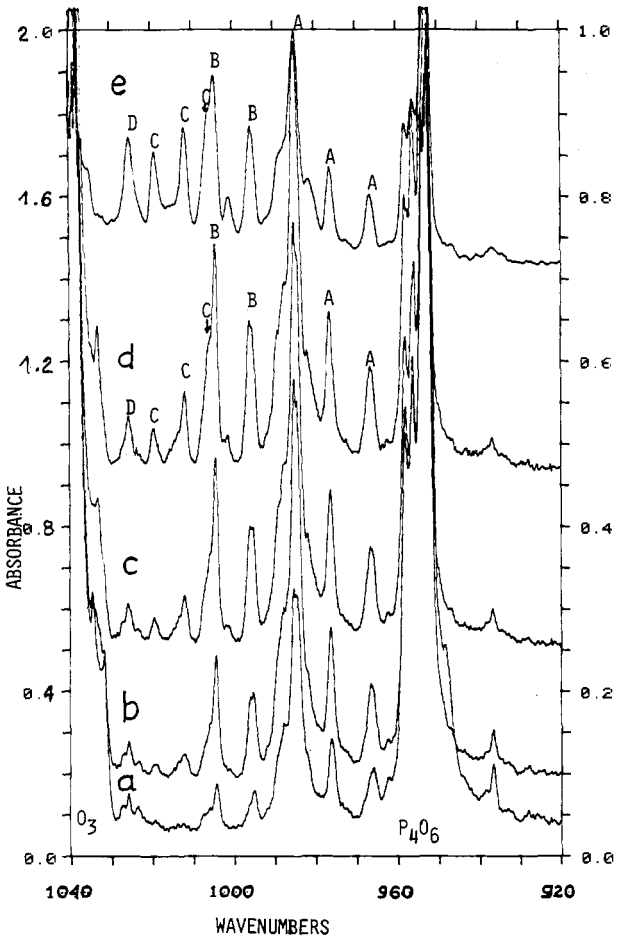

Figure 3. The 1040–920-cm^{-1} spectral region of the matrices presented in Figure 2 (a–e denote the same irradiation time). Ordinate scale is multiplied by 2 as compared for the P═O stretching region.

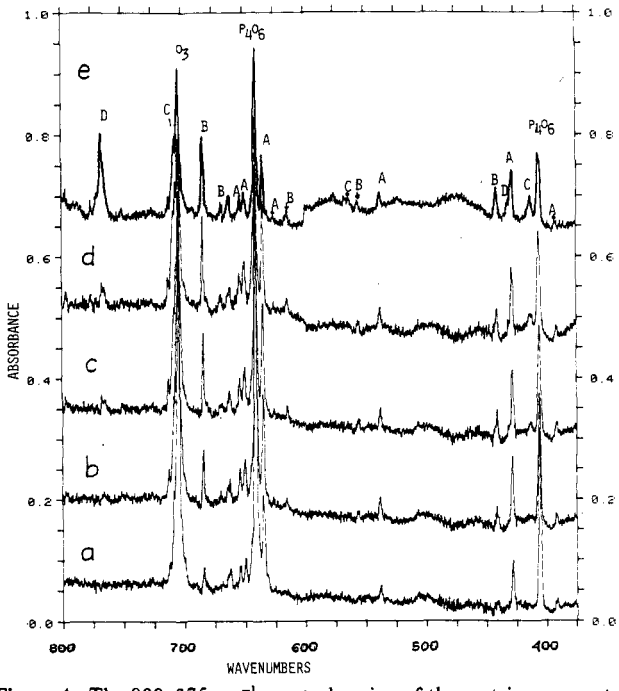

Figure 4. The 800–375-cm^{-1} spectral region of the matrices presented in Figure 2 (a–e denote the same irradiation time).

1397.8, 1401.6, 1407.9, and 1422.4 cm^{-1}; detailed analysis of the bands and spectral subtraction allow identification of another band at 1406.4 cm^{-1} overlapping with the 1407.9-cm^{-1} band. As can be seen in Figures 2a and 5a, only three bands at 1379.4, 1384.7, and 1401.6 cm^{-1} appear in the spectra of matrices when the overall

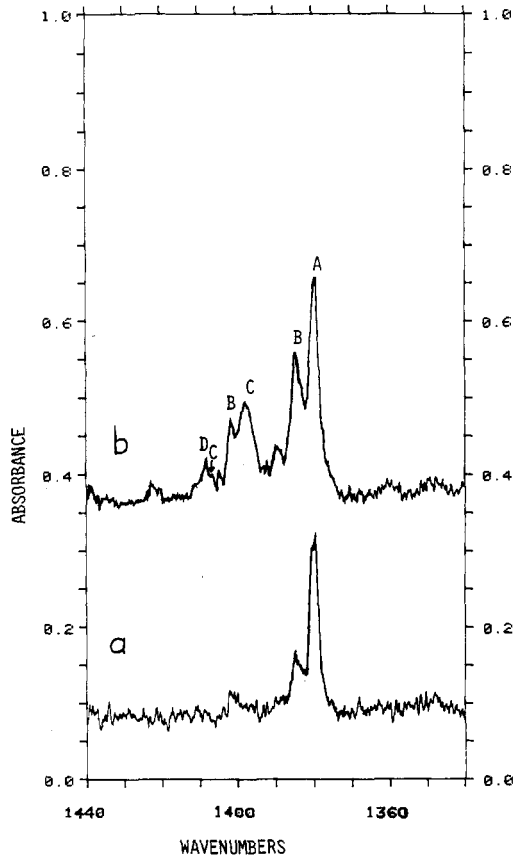

Figure 5. P═O stretching region in the spectra of matrices obtained by codeposition: Ar/P_4O_6 with Ar/O_2 = 100/1 subjected to low-power discharge (a); Ar/P_4O_6 with Ar/O_2 = 50/1 subjected to high-power microwave discharge (b).

oxygen atom concentration is kept relatively low during P_4O_6 + O reaction (low O_3 concentration, short photolysis time with 420-nm filter cutoff in the first set of experiments, and low O_2 concentration mixture subjected to low-power discharge in the second set of experiments). The strongest band at 1379.4 cm^{-1} indicated as A in Figures 2 and 5 is assigned to P_4O_7. The band is broadened by a shoulder at 1380.7 cm^{-1}, which could be due to the presence of molecular oxygen or ozone in the matrix.

The two bands at 1384.7 and 1401.6 cm^{-1} indicated as B in Figures 2 and 5 show the same relative intensity in all spectra studied and are assigned to the P_4O_8 oxide. The relative intensities of these two bands increase in comparison with the 1379.4-cm^{-1} band with prolonged photolysis time. When the overall concentration of oxygen atoms during the P_4O_6 + O reaction increases (prolonged photolysis time or high-power discharge of Ar/O_2 = 50/1 mixture), three other bands appear at 1397.8, 1407.9, and 1422.4 cm^{-1}. The relative intensity of the 1397.8/1407.9-cm^{-1} bands decreases with prolonged photolysis time, and the 1397.8-cm^{-1} band is assigned to P_4O_9 oxide, whereas the 1407.9-cm^{-1} band is assigned to the P_4O_{10} oxide. Laser ablation of solid P_4O_{10} into a condensing argon stream produced strong, sharp bands at 1408, 1026, and 768 cm^{-1} and a sharp, weak band at 577 cm^{-1},[17] which confirms the present identification of molecular P_4O_{10}. Spectral substraction shows that the 1397.8-cm^{-1} band probably has another weaker component at 1406.4 cm^{-1}, which appears as a shoulder on the 1407.9-cm^{-1} band in the spectra of matrices containing a relatively high proportion of P_4O_9. The weak 1422.4-cm^{-1} band could be due to P_4O_9 or P_4O_{10}, the corresponding absorption was not observed in laser ablation experiments of solid P_4O_{10}, and so the band is probably due to a combination band of the P_4O_9 oxide (412 + 1019 = 1431 cm^{-1}). The two weak bands appearing in the P═O stretching region at 1362.2 and 1390.1 cm^{-1} correlate with the bands due to P_4O_7 and P_4O_8

(17) McCluskey, M.; Andrews, L., to be published.

TABLE II: Symmetry and Infrared Activity for the Species P_4O_{6-10} Vibrations[a]

	P_4O_6	P_4O_7	P_4O_8	P_4O_9	P_4O_{10}
symmetry	T_d	C_{3v}	C_{2v}	C_{3v}	T_d
Γ terminal stretch		A_1	$A_1 + B_2$	$A_1 + E$	$A_1^* + F_2$
Γ terminal bend		E	$A_1 + A_2^* + B_1 + B_2$	$A_1 + A_2^* + 2E$	$E^* + F_1^* + F_2$
	$2A_1^*$	$2A_1$	$2A_1$	$2A_1$	$2A_1^*$
Γ cage	$2E^*$	2E	$2(A_1 + A_2^*)$	2E	$2E^*$
	$2F_1^*$	$2(A_2^* + E)$	$2(A_2^* + B_1 + B_2)$	$2(A_2^* + E)$	$2F_1^*$
	$4F_2$	$4(A_1 + E)$	$4(A_1 + B_1 + B_2)$	$4(A_1 + E)$	$4F_2$

[a] Asterisks denote modes inactive in the IR spectrum.

species and are most probably due to molecular aggregates formed by these oxides and P_4O_6.

As indicated in Table II, the P_4O_7 and P_4O_{10} are each predicted to show one infrared-active terminal stretching mode, while P_4O_8 and P_4O_9 should each show two. The P_4O_7 species is characterized by one band at 1379.4 cm^{-1} (A_1) and P_4O_{10} by one absorption at 1407.9 cm^{-1} (F_2).

P_4O_8 and P_4O_9 are each characterized by two absorptions at 1387.7, 1401.6 and 1397.8, 1406.4 cm^{-1}, respectively. The higher frequency and less intense bands at 1401.6, 1406.4 cm^{-1} in spectra of both molecules are assigned to symmetric P═O stretching, A_1 type modes. First, a simple bond–dipole model predicts that the symmetric P═O stretches should be less intense than the antisymmetric stretches for the angles of ca. 106° between the terminal P═O groups.[18] Second, in the P_4O_{10} species the terminal A_1 mode lies above the F_2 frequency.[4] The lower frequency and more intense bands at 1384.7, 1397.8 cm^{-1} are therefore assigned to antisymmetric P═O stretches, the 1384.7-cm^{-1} vibration in P_4O_8 is assigned to a B_1 type mode, and the 1397.8-cm^{-1} vibration in P_4O_9 is assigned to an E type mode. The 1397.8-cm^{-1} band in the studied spectra is considerably broadened in comparison with the other bands, which may be due to partial lifting of degeneracy of the E type mode. In As_4O_{7-10} oxides, the As═O stretching modes were similarly identified; the bands due to terminal A_1 modes are less intense and lie above the bands due to antisymmetric As═O stretching modes.[19]

In addition to P═O stretching, P═O bending modes (which can be mixed with cage vibrations) are also expected for terminal P═O groups. Three bands in the low-frequency region at 537.5, 556.0, and 563.4 cm^{-1} are assigned to P═O bending vibrations. The 537.7-cm^{-1} band correlates well with the 1379.4-cm^{-1} absorption and is assigned to P_4O_7 species, whereas the 556.0-, 563.4-cm^{-1} bands are assigned to P_4O_8, P_4O_9 species, respectively. These three bands appear in the region of P_4O_6 cage modes (562 cm^{-1} in P_4O_6, 553 cm^{-1} in P_4O_{10})[4] and P═O bending modes (F_2) in P_4O_{10} (573 cm^{-1}).[3] These bands could be due to A_1 cage modes in molecules of C_{3v}, C_{2v} symmetry or to a mode with a major contribution of P═O bending coordinate (which can be mixed with P_4O_6 deformation). The bands are rather assigned to a P═O bending mode which can be correlated with the 573-cm^{-1} F_2 mode in P_4O_{10}. First, the A_1 vibration has a very similar frequency in P_4O_6 and P_4O_{10}, whereas the observed band appears at 537.5 cm^{-1} in the spectrum of P_4O_7 and is shifted to 563.4 cm^{-1} in the spectrum of P_4O_9. The blue shift is consistent with the position of the corresponding mode in P_4O_{10} (573 cm^{-1}).[3] The 2.6-cm^{-1} ^{18}O isotopic shift (see Table I) for the 537.5-cm^{-1} band also supports its assignment to a mode with a large contribution of P═O bending coordinate, as the effect of ^{18}O substitution on the cage modes is very small (even on the P_4O_6 stretching modes).

^{18}O Species. Figure 6 shows infrared spectra in the P═O stretching region for the matrix obtained by codeposition of Ar/P_4O_6 and $Ar/^{18}O_3$ = 100/1 samples after 20-min full arc irradiation with 420-nm cutoff (Figure 6a), followed by 10-, 20-, and 30-min irradiation with full arc (Figure 6b–d, respectively). Similar evolution of the spectra is observed as in the case of Ar

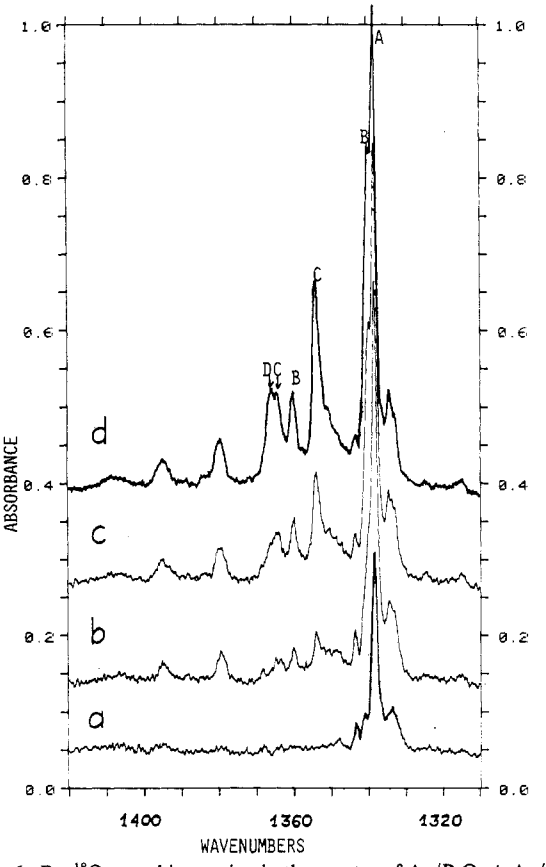

Figure 6. P═^{18}O stretching region in the spectra of $Ar/P_4O_6 + Ar/^{18}O_3$ matrix after 20-min full arc irradiation with a 420-nm filter (a) and after 10-, 30-, 60-min irradiation with full arc (b–d). $^{18}O_3$ was prepared from 98% ^{18}O-enriched gas.

$+ P_4O_6 + {}^{16}O_3$ matrices, and the bands are assigned to $P_4O_6{}^{18}O_{1-4}$ oxides on the basis of the relative intensity changes with prolonged photolysis time. The strong 1338.2-cm^{-1} band appearing after short photolysis time is due to the P═^{18}O stretch of the $P_4O_6{}^{18}O$ species and corresponds to the 1379.4-cm^{-1} P═O stretching mode in P_4O_7. The 41.2-cm^{-1} ^{18}O isotopic shift is less than the 52.0-cm^{-1} ^{18}O shift predicted for a harmonic P—O oscillator, which indicates coupling between the P═O vibration and stretching motions of the cage atoms.

The bands at 1339.8, 1359.9 cm^{-1} are assigned to $P_4O_6{}^{18}O_2$ species and correspond to the B_2, A_1 absorptions at 1384.7, 1401.6 cm^{-1}, in P_4O_8 showing 44.9-, 41.7-cm^{-1} ^{18}O shifts, respectively. The small separation between these two P═O stretching modes in ^{16}O and ^{18}O oxides indicates slight coupling between the P═O oscillators. The $P_4O_6{}^{18}O_3$ oxide is characterized by two absorptions at 1353.8, 1364.2 cm^{-1}, which show 44.0- and 42.2-cm^{-1} ^{18}O shifts as compared to their E, A_1 counterparts at 1397.8, 1406.4 cm^{-1} in P_4O_9. The 1365.6-cm^{-1} band corresponds to the $P_4O_6{}^{18}O_4$ species and exhibits a 42.3-cm^{-1} ^{18}O shift. The small difference in ^{18}O isotopic shifts between the antisymmetric and symmetric P═O stretching modes in P_4O_8 (3.2 cm^{-1}) and P_4O_9 (1.8 cm^{-1}) evidences the weak coupling between the two or three P═O stretches that occur across P—O—P bridges. The two weak bands at 1334.3, 1332.9 cm^{-1}, which occur on the low-frequency side

(18) Wilson, Jr., E. B.; Decius, J. C.; Cross, P. C. *Molecular Vibrations*; McGraw-Hill: New York, 1955.
(19) Brisdan, A. K.; Gomme, R. A.; Ogden, J. S. *J. Chem. Soc., Dalton Trans.* **1986**, 2725.

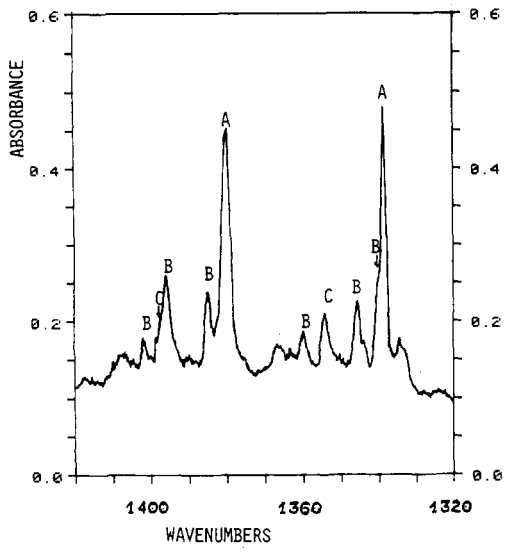

Figure 7. P=O stretching region in the infrared spectrum of the $Ar/P_4O_6 + Ar/^{16,18}O_3$ = 100/1 matrix after 30-min full arc irradiation. $^{16,18}O_3$ prepared from 55% ^{18}O-enriched gas.

of the 1338.2-cm^{-1} band and correlate with $P_4O_6{}^{18}O$ species, can be due to P=^{18}O stretch perturbed by interaction of $P_4O_6{}^{18}O$ molecule with molecular oxygen, $^{18}O_2$. The P=O stretch in the P_4O_7 species is very sensitive to the environment; it occurs at 1379.3 cm^{-1} in argon-isolated P_4O_7, but the corresponding band is reported at 1362 cm^{-1} in the infrared spectrum of P_4O_7 in a CS_2 solution and at 1328 cm^{-1} in the Raman spectrum of P_4O_7 crystal.[10] The 1379.3-cm^{-1} band occurring in the $^{18}O_3$ experiment is partly due to P_4O_7 as a small amount of ^{16}O was present in the $^{18}O_3$ sample, but a contribution from rearrangement of terminal and cage oxygen atoms cannot be excluded.

One experiment was performed with scrambled ozone ($^{16,18}O_3$). Figure 7 shows the infrared spectrum of the matrix obtained from an Ar/P_4O_6 and $Ar/^{16,18}O_3$ sample after 30-min full arc irradiation. All the bands observed in the $^{16}O_3$, $^{18}O_3$ experiments appeared in the spectrum, and two additional bands were observed at 1345.4, 1395.5 cm^{-1}. Evolution of the spectrum with prolonged photolysis (10, 20, and 30 min) shows that additional bands correlate with the bands due to P_4O_8 and $P_4O_6{}^{18}O_2$ species, and consequently they are assigned to $P_4O_6{}^{16}O^{18}O$ molecules. The appearance of the 1395.5-cm^{-1} band at 3 cm^{-1} *above* the average of the A_1 and B_2 modes for P_4O_8 with the 1345.4-cm^{-1} band 4 cm^{-1} below the average of the corresponding bands for $P_4O_6{}^{18}O_2$ indicates slight coupling between these two P=O oscillators. In fact the upper band is an almost pure P=^{16}O stretch and the lower band an almost pure P=^{18}O stretch; a harmonic oscillator calculation predicts a 52.6-cm^{-1} isotopic shift, whereas 50.3 cm^{-1} was observed. The amount of the species with three terminal oxygen atoms in the studied matrices was relatively small, and the bands due to $P_4O_8{}^{18}O$, $P_4O_7{}^{18}O_2$ mixed isotopic species were not observed.

The spectra of photolyzed Ar + P_4O_6 + $^{18}O_3$ matrices provide evidence that the reaction channel for the P_4O_6 system involves attachment of one to four oxygen atoms to trivalent phosphorus atoms of P_4O_6. This is confirmed by the strong, well-defined bands in the P=^{18}O stretching region due to $P_4O_6{}^{18}O$, $P_4O_6{}^{18}O_2$, $P_4O_6{}^{18}O_3$, and $P_4O_6{}^{18}O_4$, which are the products of the P_4O_6 + ^{18}O reaction. The presence of $P_4O_6{}^{16}O$ and $P_4O_6{}^{16}O^{18}O$ species in the $^{18}O_3$ experiments may indicate that intramolecular rearrangement between the bridged and terminal oxygen atoms occurs to a small extent as a secondary reaction.

Finally, the evolution of absorptions for the P_4O_{7-10} species in these experiments matches spectra produced by flowing discharged Ar/O_2 at varying concentrations over red phosphorus and condensing the gas mixture at 12 K.[20]

(20) Burkholder, T. R.; Andrews, L., to be published.
(21) Jenny, S. N. Ph.D. Thesis, Southampton University, Southampton, U.K., 1981.

Cage Modes

Since there is no considerable mixing between the P=O vibrations and the P_4O_6 cage modes, there should be good correlation between the P_4O_6 modes of P_4O_{7-10} species and the vibrations of the P_4O_6 molecule. Attachment of one or three oxygen atoms lowers the symmetry of the P_4O_6 cage from T_d to C_{3v} while the attachment of two oxygen atoms lowers the symmetry to C_{2v}, and the splitting and/or activation of cage modes should follow the correlation diagram between the T_d, C_{3v}, and C_{2v} point groups (see Table II).

Figures 3 and 4 show the spectra of $Ar/P_4O_6/^{16}O_3$ matrices after photolysis in the region of the cage modes. The frequencies of the bands correlating with the 952.7-cm^{-1} mode of P_4O_6 (appearing in the region 1040–960 cm^{-1}) were not reproducible after different photolysis steps; they varied within 1 wavenumber, which was possibly due to different amounts of molecular oxygen trapped in the matrix. The other bands showed good reproducibility. The assignment of these bands to specific higher oxides was made by correlating their intensities with corresponding absorptions in the P=O stretch region. The cage modes of P_4O_7 are identified at 984.8, 976.3, 966.4, 653.5, 649.6, 634.6, 427.6, and 391.0 cm^{-1}. The 984.8-, 976.3-, and 966.4-cm^{-1} bands correlate with the 919-cm^{-1} F_2 mode of P_4O_6 while the 653.5-, 649.6-, and 634.6-cm^{-1} bands occur in the vicinity of the 643-cm^{-1} F_2 mode of P_4O_6. There are three shoulders on the strong 984.8-cm^{-1} absorption at 988.9, 987.1, and 981.6 cm^{-1}, which are probably due to different matrix sites. Two P_4O_7 bands at 427.6 and 391.0 cm^{-1} appear in the region of 407.0-cm^{-1} F_2 deformation modes of P_4O_6. The activated A_1 band corresponding to the 613-cm^{-1} A_1 band in P_4O_6 is identified at 625.9 cm^{-1}. The splitting of the two higher frequency F_2 modes of the P_4O_6 cage into three components in the P_4O_7 species may indicate that the C_{3v} symmetry of the isolated molecule is lowered due to the matrix environment, and the degeneracy of the E mode is lifted (see Table I). The observed frequencies of P_4O_7 species are in good agreement with the reported analytical Raman data for P_4O_7.[10]

The cage modes of P_4O_8 were identified at 1004.3, 995.9, 683.7, 669.3 (the latter with somewhat less confidence), and 440.4 cm^{-1} in the vicinity of the three F_2 modes of P_4O_6 molecule, and one band was observed at 614.5 cm^{-1} close to the A_1 mode of P_4O_6 at 613 cm^{-1}. The absorptions due to P_4O_9 cage modes are identified at 1019.4, 1011.9, 1005.7, 706, and 431 cm^{-1} and can also be correlated with the three F_2 modes of P_4O_6. Three bands due to the F_2 cage modes of P_4O_{10} were identified at 1025.5, 766.9, and 412 cm^{-1}, which correspond to the most intense bands reported in the spectra of solid P_4O_{10}[3] and from YAG laser ablated P_4O_{10}.[17]

The cage modes in the $P_4O_6{}^{18}O_{1-4}$ species were also identified in the spectra of photolyzed Ar + P_4O_6 + $^{18}O_3$ matrices, and the corresponding frequencies are reported in Table I. As one may notice, the changes in frequencies of the cage modes due to ^{18}O substitution in the terminal groups are less than 5 cm^{-1}, which indicates that the terminal P=O vibrations have little effect on vibrations involving the 10 cage atoms.

The bands identified for P_4O_6 cage motion in P_4O_{7-10} oxides are assigned to the vibrations correlating with $3F_2$ and A_1 vibrations in P_4O_6, which give rise to the most intense bands observed in infrared ($3F_2$) and Raman spectra (A_1) of the P_4O_6 molecule. The band due to the second A_1 mode was weak in the reported Raman spectrum of gaseous P_4O_6 and the two Raman-active E modes were not observed; the bands due to the corresponding modes in the spectra of P_4O_{7-10} oxides are probably also too weak to be observed in the studied matrices.

It is interesting to notice that the frequencies of the two F_2 modes of P_4O_6 (953, 641 cm^{-1}) increase continuously (see Table I) when going from P_4O_7 to P_4O_{10}. This trend correlates with the structure of the P_4O_{6-10} oxides. The longer P^{III}—O (P^{III}) and P^{III}—O (P^V) bonds in P_4O_6, P_4O_7 are gradually replaced by shorter P^V—O(P^{III}) and P^V—O(P^V) bonds in P_4O_9, P_4O_{10},[11] the P^V—O(P^V) bond being characterized by higher force constant than the P^{III}–O(P^{III}) bond. In the bridge-bonded P_4O molecule, which has been recently isolated an argon matrix,[12] the antisymmetric and symmetric P—O—P stretching modes were identified at 856

and 553 cm^{-1}, just below the two most intense F_2 modes of P_4O_6. One may expect that the intermediate bridge-bonded oxides P_4O_{2-5} (which have not been synthesized as yet) will show strong absorptions characteristic of P—O—P antisymmetric and symmetric stretchings in the 856–953- and 553–641-cm^{-1} regions, respectively.

Conclusions

Matrix reaction of P_4O_6 with ^{16}O or ^{18}O atoms (obtained from ozone photolysis and discharge of oxygen) leads to formation of P_4O_{7-10} and $P_4O_6{}^{18}O_{1-4}$ oxides, respectively. The spectra of the four higher oxides are interpreted on the basis of a central P_4O_6 cage structure with appropriate numbers of $P{=}^{16}O$ or $P{=}^{18}O$ bonds. The $P{=}^{16}O$, $P{=}^{18}O$ vibrations are identified and assignments are proposed for several of the more intense P_4O_6 cage absorptions. The isotopic shifts of the P=O stretching vibrations give evidence for some coupling to cage motions and between the P=O stretching vibrations across the P—O—P bridges.

Acknowledgment. We gratefully acknowledge financial support from NSF Grant CHE85-16611, the gift of a P_4O_6 sample prepared by J. L. Mills from Texas Tech University, and a report of phosphorus oxide studies[21] provided by J. S. Ogden.

Note Added in Proof. An excellent combined mass spectroscopic/matrix isolation infrared study on the P_4O_{6-10} molecular species including ^{18}O substitution has just come to our attention.[21] The stable compounds P_4O_6 and P_4O_{10} were prepared and condensed with excess argon. Reported fundamentals are in excellent (± 2 cm^{-1}) agreement with those reported here except for the strong F_2 fundamental of P_4O_{10} observed here at 1408 cm^{-1} and in Southampton at 1403 cm^{-1}. The mass spectroscopic experiment was especially valuable for monitoring the intermediate oxide species evaporating into the matrix sample. Matrix spectra of P_4O_7 and P_4O_8 recorded by Jenny and Ogden are in excellent agreement with those reported here except that reagent ozone masked any weak 708- and 703-cm^{-1} absorption in the Virginia study.

Registry No. P_4O_6, 12440-00-5; P_4O_7, 12065-80-4; P_4O_8, 70983-17-4; P_4O_9, 12037-11-5; P_4O_{10}, 16752-60-6; ^{16}O, 17778-80-2; ^{18}O, 14797-71-8; Ar, 7440-37-1.

Enhanced Raman Spectroscopy at Dielectric Surfaces

Dennis J. Walls and Paul W. Bohn*

Department of Chemistry, University of Illinois at Urbana-Champaign, 1209 W. California St., Urbana, Illinois 61801 *(Received: July 1, 1988)*

We present enhanced Raman scattering results from a new type of structure, typically consisting of 60 Å of SiO_2 sputtered on Ag or Au island films, all coated on a lithographically defined opening in a masked SiO_2 substrate. Total internal reflection in the SiO_2 substrate is used to excite plasma resonances in the island films with higher incident field amplitudes than possible with external excitation, which in turn enhance scattering from molecules bound to the outer SiO_2 surface. Evidence for long-range enhancement comes from chemical passivation, scanning Auger, and distance dependence experiments, as well as from comparing coated with uncoated Au islands. The dependence of scattering on excitation angle can be interpreted in terms of the strengths of the evanescent field components at the substrate/metal interface, while the wavelength dependence agrees with behavior predicted by the optical properties of the island films for both Ag and Au. Implications for determination of adsorbate orientation are discussed.

Introduction

Surface modification has come to play an important role in a large number of technologies, including catalysis, adhesion, lubrication, corrosion inhibition, and chemical separations. The useful characteristics provided by surface functionalization are related to surface structure, underscoring the importance of developing probes to correlate changes in material function with surface structure. Vibrational spectroscopy is a powerful tool for surface characterization studies, since it provides detailed information about the way a molecule is bound and situated in its surroundings.[1,2] Raman spectroscopy is extremely attractive for such measurements, since it allows for in situ experiments under diverse conditions.[3] Raman measurements of monomolecular layers on solid supports are, however, extremely difficult to make. Most successful approaches to obtain surface Raman information enhance the Raman scatter from the surface-bound species.[4] Since the first observation of the effect in 1974[5] and the subsequent recognition of the actual nature of the enhancements in 1977,[6,7] SERS has attracted a flurry of experimental and theoretical activity.[8-10]

Despite having submonolayer sensitivity, the application of SERS to general surfaces has been limited, because signal enhancement is restricted to adsorbates on a small subset of specially prepared metal surfaces. Comparatively little effort has been made to extend SERS to nonmetallic surfaces, focusing mainly on adsorbates on metal oxide surfaces, either incorporated into tunnel junctions[11,12] or separated from a SERS enhancing Ag overlayer by CaF_2 overlayers.[13] In addition, silver island films have been used as overlayers to enhance the Raman spectra of surfaces and surface-bound species.[14-16] While all these methods can preserve

* Author to whom correspondence should be addressed.

(1) Bolger, B. In *Surface Studies with Lasers*; Ausseneg, F. R., Leitner, A., Lippitsch, M. E., Eds.; Springer-Verlag: Berlin, 1983; p 1.
(2) Willis, R. F. In *Vibrational Spectroscopy of Adsorbates*; Willis, R. F., Ed.; Springer-Verlag: Berlin, 1980.
(3) Wokaun, A. *Mol. Phys.* **1985**, *56*, 1.
(4) Campion, A. *Comments Solid State Phys.* **1984**, *11*, 107.
(5) Fleischmann, M.; Hendra, P. J.; McQuillan, A. J. *Chem. Phys. Lett.* **1974**, *26*, 163.
(6) Jeanmaire, D. L.; Van Duyne, R. P. *J. Electroanal. Chem.* **1977**, *84*, 1.
(7) Albrecht, M. G.; Creighton, J. A. *J. Am. Chem. Soc.* **1977**, *99*, 5215.
(8) Chang, R. K.; Furtak, T. E., Eds. *Surface Enhanced Raman Scattering*; Plenum: New York, 1982.
(9) Moskovits, M. *Rev. Mod. Phys.* **1985**, *57*, 783.
(10) Murray, C. A. In *Advances in Laser Spectroscopy*; Garetz, B. A., Lombardi, J. R., Eds.; Wiley: New York, 1986; Vol. 3, p 49.
(11) Tsang, J. C.; Kirtley, J. R.; Theis, T. N.; Jha, S. S. *Phys. Rev. B* **1982**, *25*, 5070.
(12) Tsang, J. C.; Avouris, P.; Kirtley, J. R. *J. Chem. Phys.* **1983**, *79*, 493.
(13) Murray, C. A.; Allara, D. L.; Rhinewine, M. *Phys. Rev. Lett.* **1981**, *46*, 57.
(14) Parry, D. B.; Dendramis, A. L. *Appl. Spectrosc.* **1986**, *40*, 656.

0022-3654/89/2093-2976$01.50/0